Aquaculture 599 (2025) 742111

Contents lists available at ScienceDirect

Aquaculture

journal homepage: www.elsevier.com/locate/aquaculture

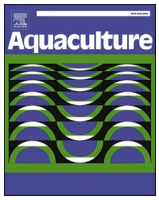

Differential responses of an economically important macroalga and a bloom-forming microalga to marine heatwaves in a coculture system

Xin Zhao [a,1], Lin Gao [a,1], Xu Li [a], Gang Li [b], Guang Gao [a,*]

[a] State Key Laboratory of Marine Environmental Science & College of Ocean and Earth Sciences, Xiamen University, Xiamen 361102, China
[b] Key Laboratory of Tropical Marine Bio-Resources and Ecology, South China Sea Institute of Oceanology, Chinese Academy of Sciences, Guangzhou 510530, China

ARTICLE INFO

Keywords:
Algal competition
Harmful algal bloom
Marine heatwave
Seaweed aquaculture
Transcriptomics

ABSTRACT

Harmful algal blooms can impose severe harm to aquatic ecosystems. Macroalgae cultivation has been demonstrated to inhibit the occurrence of harmful algal blooms. However, our understanding of how marine heatwaves (MHWs) affect the competition dynamics between cultivated macroalgae and bloom-forming microalgae remains limited. In this study, a widely cultivated macroalga *Gracilariopsis lemaneiformis* and a common bloom-forming microalga *Skeletonema costatum* were co-cultured under a simulated MHW event. The negative effects of MHW on relative growth rate (RGR) and net photosynthetic rate (NPR) of *G. lemaneiformis* increased with culture time until the end of one week of recovery. MHW also induced higher dark respiration rate (DRR) in *G. lemaneiformis*. Transcriptome analysis shows that only several genes involved in fatty acid degradation (*HADH*, *echA*), glycolysis (*PFK*) and carotenoid biosyenhtesis (*PSD*) were significantly upregulated in *G. lemaneiformis* which was insufficient to deal with the stress caused by MHW. In contrast, the RGR and NPR of *S. costatum* fully recovered from the negative influences of MHW by the end of recovery period. Most genes involved in the pathways of oxidative phosphorylation (a process of generating ATP), glycolysis, TCA (tricarboxylic acid) cycle, fatty acid degradation, Calvin cycle (carbon fixation process) and nitrogen metabolism were significantly upregulated in *S. costatum*, indicating a robust self-regulation and repairing capability to cope with environmental stress. These findings suggest that when co-cultured with *G. lemaneiformis*, *S. costatum* exhibited greater resilience to MHW, conferring it a competitive advantage and enhancing the likelihood of harmful algal blooms in areas where macroalgae are cultivated.

1. Introduction

Continuous CO_2 emission is exacerbating global warming and triggering ocean acidification. In tandem with the rise in global temperatures, the incidence of extreme weather events, such as marine heatwaves (MHWs), is escalating in frequency, duration, and intensity (Oliver et al., 2018; Laufkötter et al., 2020; Yao and Wang, 2022). Intense and recurrent MHWs have been particularly observed along the coastal regions of China, the western South China Sea, and the southwestern Luzon Strait (He et al., 2023). These extreme and frequent MHWs pose a grave threat to marine ecosystems (Pecl et al., 2017). For example, MHWs can cause widespread coral bleaching, severely damaging coral reef ecosystems (Donovan et al., 2021). Both in situ investigation and laboratory experiments showed that MHWs could lead to variation of algal community composition, potentially affecting carbon fixation and sequestration (Remy et al., 2017; Du and Peterson, 2018). In addition, harmful algal blooms (HABs) can be promoted by MHWs, imposing a threat to global biodiversity (Hayashida et al., 2020; Takagi et al., 2022; Kelly et al., 2023). About a month after MHWs in the Northwest Pacific in 2021, unprecedented large-scale HABs were observed for the first time in the waters near Japan, even extending to coastal shelf waters, and persisted for three months (Kuroda and Setou, 2021).

Harmful Algal Blooms (HABs) have emerged as a global concern and toxins in toxic species can be transferred to higher trophic levels including zooplankton, shellfish, fish, marine mammals, and humans (Wells et al., 2015). Consequently, HABs exert a variety of detrimental impacts on marine ecosystems, fisheries, aquaculture, local economies, and human health and well-being (Takagi et al., 2022). Over the past two decades, there has been a notable increase in frequency, severity,

* Corresponding author.
E-mail address: guang.gao@xmu.edu.cn (G. Gao).
[1] These authors contributed equally to this work.

https://doi.org/10.1016/j.aquaculture.2024.742111
Received 24 October 2024; Received in revised form 27 December 2024; Accepted 31 December 2024
Available online 2 January 2025

and geographic spread of HABs (Anderson et al., 2021).

Macroalgae, mainly inhabit in intertidal zones, as the most important producers in coastal waters, play an essential role in coastal ecosystem maintenance and carbon sequestration (Gao et al., 2022). In addition, studies shows that some macroalgae have an inhibitory effect on HABs. For example, many species of *Gracilaria* endemic to Asian waters could inhibit the growth of many species of red tide algae through allelopathy (Ye et al., 2013; Ye et al., 2014; Yang et al., 2015). The inhibition of macroalgae on bloom-forming microalgae can also improve phytoplankton diversity (Chai et al., 2018). Asia has a long history of seaweed aquaculture. Red tides seldom occur in seaweed aquaculture areas due to the competition and allelopathic inhibition of macroalgae. However, it was reported that red tides occurred in seaweed aquaculture areas in recent years (Li et al., 2022). Whether MHWs led to the competitive changes between macroalgae and bloom-forming microalgae warrants further investigation. Previous studies have predominantly centered on individual responses to MHWs (Jiang et al., 2022; Smith et al., 2023; Fischer et al., 2024). While a recent study indicated that MHWs might augment the competitive edge of *S. costatum* over *G. lemaneiformis*, the underlying molecular mechanisms remain elusive (Gao et al., 2024). Concurrently, how the co-cultured macroalgae and microalgae respond to MHWs needs to be further studied.

As a red macroalga with extensive economic and ecological restoration values, *G. lemaneiformis* exhibits the merits of robust temperature adaptability and rapid growth, so it is widely cultured along the coasts of China, spanning from North to South (Fei, 2004; Gao et al., 2022). As a representative phytoplankton species with global distribution, large-scale blooms are dominated by *S. costatum* under certain environmental conditions (Wang et al., 2006). It is also the most frequent red tide diatom in China (Feng et al., 2024). Previous studies show that *G. lemaneiformis* has a substantial inhibitory effect on *S. costatum* (Yang et al., 2015; Gao et al., 2024). We hypothesize that this competition dynamic could be altered by MHW. In this study, *G. lemaneiformis* and *S. costatum* were cocultured under a simulated MHW, and both physiological and transcriptome data were analyzed to test the hypothesis and to explore the potential mechanisms.

2. Materials and methods

2.1. Algal collection and algae culture

Gracilariopsis lemaneiformis was collected from a macroalgae culture area in Sansha Bay, Ningde City, Fujian Province in February 2022 (119.31°E, 26.39°N), and transported back to the laboratory in the condition of low temperature (around 15 °C) and dark. After that, natural seawater filtered by a 0.22 μm pore size filter was used to repeatedly clean the algae to remove surface attachments. The cleaned thalli were placed in an incubator (HP200G-3 light incubator, Ruihua, Wuhan, China), with the temperature set at 17 °C and the light intensity set at 70 μmol·photons·m^{-2}·s^{-1} (light: dark = 12: 12), and cultivated with f/2 medium for at least one week. Before the experiment, *G. lemaneiformis* thalli with similar branch length were selected and attached other algae were removed as much as possible with degreased cotton. Subsequently, the thalli were treated with 4 % streptomycin antibiotics (400 U·mL^{-1} penicillin and 0.4 mg·mL^{-1} streptomycin), and placed in a light incubator for at least 48 h to reduce pollution of microalgae and bacteria, and then washed repeatedly with sterilized seawater to wash off the antibiotics.

Skeletonema costatum (*Cleve 1900*) was taken from the Center for Collections of Marine Algae (CCMA), the State Key Laboratory of Marine Environmental Science of Xiamen University. *Skeletonema costatum* was also treated with double antibodies (streptomycin, the final concentration was 200 U·mL^{-1} penicillin, 0.2 mg·mL^{-1} streptomycin) for 24 h before the experiment, and the conditions of temperature and light were consistent with those of *G. lemaneiformis* culture.

2.2. Experimental design

The seawater used in the experiment was natural seawater collected from coastal area of Jinjiang city (118.60°E, 24.52°N), Fujian province of China, which was filtered by a 0.22 μm filter membrane and then sterilized by an autoclave at 106 °C. The concentrations of dissolved inorganic nitrogen (DIN) and dissolved inorganic phosphorus (DIP) in natural seawater were 10 μmol·L^{-1} and 0.5 μmol·L^{-1}, respectively. The *G. lemaneiformis* and *S. costatum* were simultaneously cultured in a triangle conical bottle with a capacity of 1 L filled with 1 L sterilized seawater, f/2 medium was added, and outdoor air filtered by a 0.22 μm filter membrane was filled for culture. Medium was renewed half every three days for a semicontinuous culture to supply enough nutrients (Fig. S1). Light intensity was 70 μmol·photons·m^{-2}·s^{-1} with a light: dark cycle of 12 h: 12 h. Original concentrations of *G. lemaneiformis* and *S. costatum* were 1 g·L^{-1} and 1 × 10^4 cell·mL^{-1} respectively, which represented the culture density of *G. lemaneiformis* and the biomass density of *S. costatum* when it bloomed (Gao et al., 2024). The control group (17 °C Baseline, 17 °C BL) and the heatwave treatment group (20 °C Heatwave, 20 °C HW) were set in the experiment. Four repetitions were set for each treatment. The baseline temperature represents the spring temperature in the *G. lemaneiformis* cultivation area and the 3 °C heatwave can occur in coastal waters of China (Yao and Wang, 2022; Jiang et al., 2024). The control group's temperature was set at 17 °C, which was fixed, while the heatwave treatment group simulated the process of marine heatwave by artificially regulating the temperature (Fig. 1). The heatwave group increased from 17 °C to 20 °C at a rate of 0.5 °C per day. The heating process lasted for 6 days, which was termed heating period. Then it was kept at 20 °C for one week, which was termed maintenance period, and then it dropped to 17 °C at a rate of 0.5 °C per day. The cooling process also lasted for 6 days, which was termed cooling period. Afterwards it continued to be cultured at 17 °C for one week, which was the heatwave recovery period. Therefore, the total culture period was 24 days.

2.3. Measurement of relative growth rate

As for the measurement of relative growth rate of *G. lemaneiformis*, thalli were taken out from the culture bottles, wiped with absorbent paper and weighed by an analytical balance (HZK-FA110, HZ, USA) in an ultra-clean workbench.

The cell number of *S. costatum* was measured by spectrophotometer at 680 nm, and the measured light absorption value was substituted into the linear relationship between the cell number (cell·mL^{-1}) and light absorption value of *S. costatum*. The weight of *G. lemaneiformis* and the biomass of *S. costatum* were measured every three days.

The relative growth rate (RGR) of *G. lemaneiformis* and *S. costatum* were calculated according to the following formula:

$$\mathrm{RGR}\left(\%\mathrm{d}^{-1}\right) = \left(\ln \mathrm{W_t} - \ln \mathrm{W_0}\right)/\mathrm{t} \times 100\%,$$

where W_0 and W_t represent the weight of *G. lemaneiformis* on day 0 and day t or the cell number of *S. costatum* on day 0 and day t, respectively.

2.4. Measurements of net photosynthetic rate and dark respiration rate

The net photosynthetic rate (NPR) and dark respiration rate (DRR) of algae were measured by Clark-type oxygen electrode (Oxygraph+, Hansatech, UK) during the culture. A constant temperature circulator was used to maintain the temperature during measurement, which was consistent with the culture temperature set in the experiment. And the light intensity was adjusted by moving the distance between the light source and the measuring chamber, which was consistent with the light intensity in the growth incubator. For *G. lemaneiformis*, in order to eliminate the physiological differences of different algae segments, we

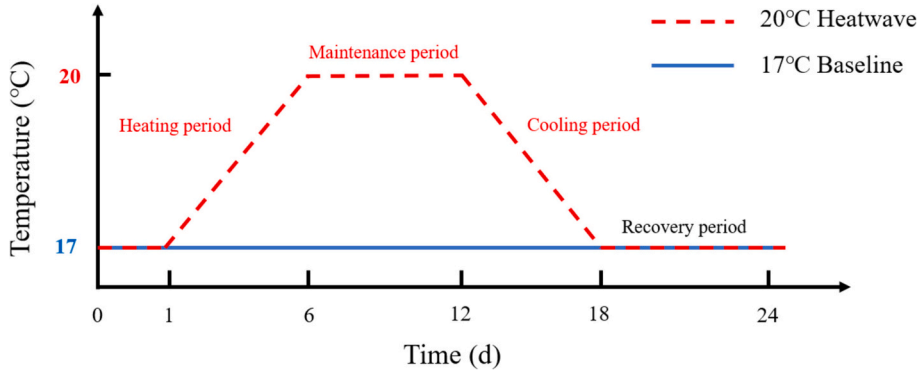

Fig. 1. Stages and temperature change of the simulated marine heatwave.

cut three sections of thalli with a length of 1–2 cm and a total weight of about 0.02 g, and then the thalli were transferred to a centrifuge tube filled with 2 mL of filtered original culture water. At the same time, before the determination, we put it under experimental conditions for at least 1 h to reduce the influence of mechanical damage on the determination of algae. As for *S. costatum*, 2 mL of cultured water was added to the measuring chamber for measurement. The NPR and DRR of two algae were both measured for 10 min. The net photosynthetic rate and dark respiration rate were expressed as μmol $O_2 \cdot g^{-1}FW \cdot h^{-1}$ for *G. lemaneiformis*, and pmol $O_2 \cdot cell^{-1} \cdot h^{-1}$ for *S. costatum*.

2.5. Measurements of photosynthetic pigments

In this experiment, the contents of Chl *a* and carotenoid in two kinds of algae were determined. For *G. lemaneiformis*, we weighed about 0.02 g (FW) of thalli in a 15 mL centrifuge tube, added 5 mL 100 % methanol to completely immerse the thalli, and stored it in the dark at 4 °C for 24 h. During the measurement, the extract was shaken evenly, then centrifuged at 8000 r/min at 4 °C for 10 min by using a high-speed freezing centrifuge (Universal 320R, Hettich, Germany). After that, the supernatant was taken and measured with an ultraviolet spectrophotometer (TU-1810DASPC, China) with 100 % methanol as reference solution.

For *S. costatum*, about 5 mL of the sample was filtered on 25 mm GF/F filters (Whatman, USA) and transferred to a 15 mL centrifuge tube. After adding 5 mL of 100 % methanol solution to immerse the membrane sample, stored it in the dark at 4 °C for 24 h. The extract was centrifuged, measured as described above.

The contents of Chl *a* and carotenoids were calculated according to the formulas of Porra et al. (Porra et al., 1989) and Strickland et al. (Strickland and Parsons, 1972) respectively:

$$\text{Chl } a \left(\mu g \cdot mL^{-1}\right) = 16.29 \times (A_{665} - A_{750}) - 8.54 \times (A_{652} - A_{750})$$

$$\text{Carotenoids } \left(\mu g \cdot mL^{-1}\right) = 7.6 \times [(A_{480} - A_{750}) - 1.49 \times (A_{510} - A_{750})]$$

where A_{750}, A_{665}, A_{652}, A_{510}, and A_{480} are the absorbance wavelength at 750, 665, 652, 510, and 480 nm, respectively. For *G. lemaneiformis*, the pigment content units were converted into $mg \cdot g^{-1}$ FW. As for *S. costatum*, the values were converted to $pg \cdot cell^{-1}$.

2.6. Measurements of POC、PON、C/N

Gracilariopsis lemaneiformis was cut off at the base and end, rinsed with sterilized seawater to wash off *S. costatum* which might be attached to the surface of the algae, and the water on the surface of the algae was absorbed by absorbent paper, then transferred to a 2 mL centrifuge tube and stored in a refrigerator at −20 °C. As for *S. costatum*, about 5 mL of cultured water was filtered on GF/F membrane that was pre-burned by muffle furnace with 450 °C for 6 h, and the pressure was controlled within 0.01 MPa to avoid the breakage of algae cells. Then it was transferred to a 2 mL centrifuge tube and stored in a refrigerator at −20 °C. Before determining the POC and PON contents of the sample, the sample was dried in an oven at 60 °C for 24 h to remove water, then put in a closed container containing concentrated hydrochloric acid with a concentration of 12 $mol \cdot L^{-1}$ for 24 h to remove particulate inorganic carbon (PIC), and then dried in an oven at 60 °C for 24 h to remove HCl. POC and PON contents were then analyzed using an elemental analyzer (vario EL cube, Germany).

2.7. Measurements of transcriptomics of G. lemaneiformis and S. costatum

The samples of *G. lemaneiformis* and *S. costatum* in the control group and the heatwave group were collected at the end of the heatwave (D18) and one week after the end of the heatwave (D24) for transcriptome determination and analysis. The two sampling points were both in the middle period of photoperiod (around 2 p.m.). About 0.1 g (FW) of *G. lemaneiformis* were collected, transferred into a sterilized 2 mL freezing tube, and immediately put in liquid nitrogen for quick freezing. For *S. costatum*, 10 mL of algae solution was filtered on a 3 μm PC membrane (25 mm, Millipore) by a vacuum pump (the pressure was controlled within 0.01 MPa), transferred to a sterilized 2 mL freezing tube, and immediately put into liquid nitrogen for quick freezing. Afterwards, both algae samples were transferred to an ultra-low temperature refrigerator at −80 °C for storage.

Both *G. lemaneiformis* tissue and *S. costatum* cell samples were sent to BGI (Shenzhen, China) for mRNA separation, enrichment, fragmentation and synthesis of double-stranded cDNA to construct a cDNA library, which was inspected by Agilent 2100 Bioanalyzer, and then sequenced by DNBSEQ platform. Clean reads were obtained by filtering out low quality, linker pollution and high content of unknown base N in the original sequenced data. Clean reads were assembled to get unigene, and then the unigene was annotated and detected by SSR, and the clean reads were compared to the reference genome sequence by Bowtie2 (v2.2.5) (Langmead and Salzberg, 2012). Then, the gene expression level of each sample was calculated and quantified using RSEM (v1.2.8) (Li and Dewey, 2011). The differential expression gene (DEG) between different samples was detected according to the method described by Michael et al. with $|\log_2 \text{Fold Change}| > 1$ and Q value < 0.05 (Jiang et al., 2024). Further cluster analysis, functional enrichment analysis and KEGG pathway analysis were carried out with the "phyper" package in R software.

2.8. Data processing and statistical analysis

The experimental data were all expressed by the mean and standard deviation ($X \pm SD$), statistically analyzed by SPPS 25 and/or R language (version 4.3.1), and plotted by Origin 2019b software and/or R language. One-way ANOVA was used to evaluate the significance of

differences between different treatments using SPSS 25. Least-Significant difference (LSD) of post hoc testing was analyzed, and the significance level was set at 0.05. Generalized additive models (GAMs) were used to emphasize patterns of physiological parameters over time by using the 'mgcv' package in R.

3. Results

3.1. Relative growth rate of G. lemaneiformis and S. costatum

The relative growth rates of *G. lemaneiformis* and *S. costatum* were monitored during a simulated heatwave (Fig. 2A&B). No significant effect of heatwave on growth of *G. lemaneiformis* was found at any time point (ANOVA, $p > 0.05$) while heatwave reduced growth of *S. costatum* on day 15 (ANOVA, $p = 0.046$) (Fig. 2A&B). Based on the analysis of generalized additive models (GAMs), the effects of heatwave on growth of *G. lemaneiformis* and *S. costatum* during the whole culture period were not significant (Fig. 2C&D, $p > 0.05$). However, the effect patterns were different between *G. lemaneiformis* and *S. costatum*. The effect of heatwave on *G. lemaneiformis* was always negative and the negative extent increased with time until the end of one-week recovery (Fig. 2C). Different from *G. lemaneiformis*, heatwave less affected the RGR of *S. costatum* was less affected by the end of heatwave and showed a positive effect after the recovery period (Fig. 2D).

3.2. Photosynthesis comparisons between G. lemaneiformis and S. costatum

Net photosynthetic rates of *G. lemaneiformis* and *S. costatum* were also measured on different days during the simulated MHW (Fig. 3A&B). Heatwave reduced net photosynthetic rate of *G. lemaneiformis* on day 24 while it reduced net photosynthetic rate of *S. costatum* on days 6 and 18 (ANOVA, $p < 0.05$). Based on GAMs analysis, the heatwave had negative effects on both *G. lemaneiformis* ($p = 0.070$) and *S. costatum* ($p < 0.001$) during the whole culture period, but the effect patterns were different (Fig. 3C&D). The negative effect of heatwave on *G. lemaneiformis* increased with the incubation time, and the negative effect became significant after the cooling period, with the highest inhibition rate reaching 30 % (Fig. 3C). In contrast, the negative effect of MHW on *S. costatum* showed a trend of first increase and then decrease. The largest negative effect (34 %) occurred on day 6 (beginning of MHW maintenance period) and then decreased to 16 % by the end of recovery period (Fig. 3D).

MHW significantly stimulated dark respiration rate of *G. lemaneiformis* on days 6 and 12 but reduced dark respiration rate of *S. costatum* on day 18 (Fig. 4 A&B, ANOVA, $p < 0.05$). Based on GAMs analysis (Fig. 4 C&D), heatwave significantly affected dark respiration rate of *G. lemaneiformis* ($p < 0.001$) while its effect on *S. costatum* was insignificant ($p = 0.849$). The stimulative effect of heatwave on dark respiration rate of *G. lemaneiformis* increased first, reached the maximum on day 9 and then decreased with culture time (Fig. 4C). Different from *G. lemaneiformis*, the effect of MHW on *S. costatum* dark respiration rate turned from positive at beginning of MHW to negative at the end of MHW (Fig. 4D). The effect range (−5 %–10 %) for *S. costatum* was narrower than that (0–25 %) for *G. lemaneiformis*, suggesting that MHW had more severe effects on *G. lemaneiformis* than *S. costatum*.

3.3. Photosynthetic pigments content

Heatwave reduced Chl *a* content in *G. lemaneiformis* on day 24 (ANOVA, $p = 0.022$) but did not show significant effect on Chl *a* content in *S. costatum* (Fig. 5A&B). Based on GAMs analysis, the effect of MHW

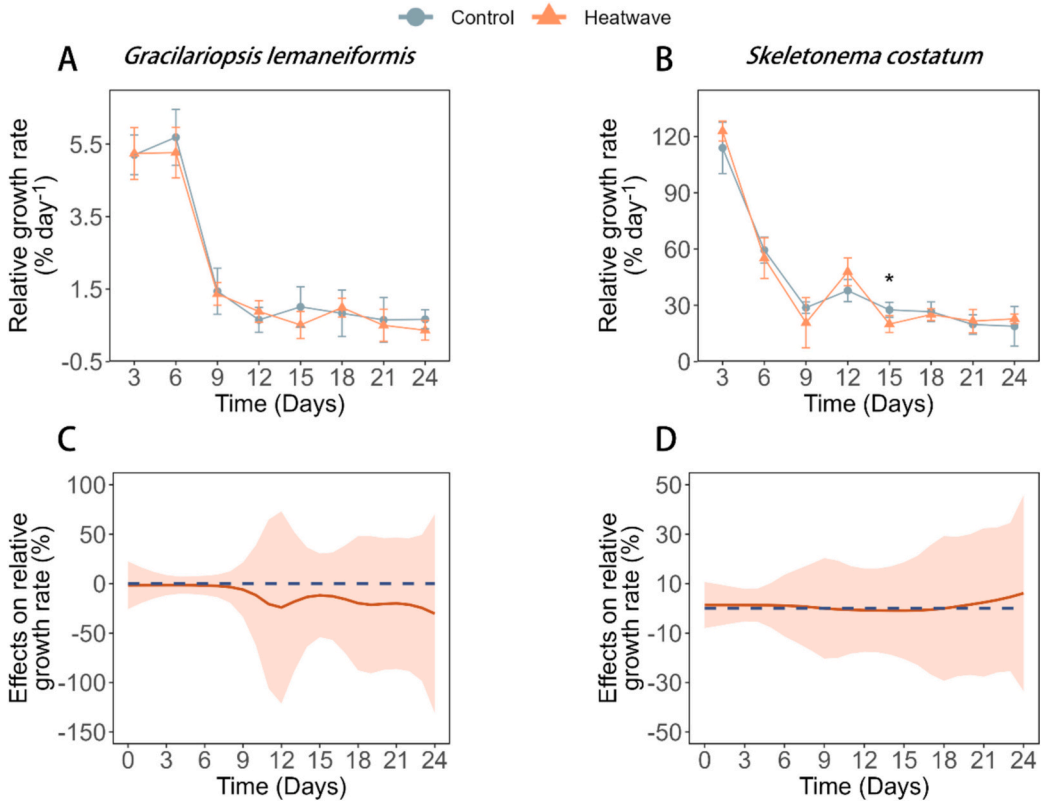

Fig. 2. The relative growth rate (RGR) of *G. lemaneiformis* (A) and *S. costatum* (B) under control and heatwave conditions. The value is mean ± standard deviation (SD), and * indicates that there is a significant difference between the control and the heatwave groups ($p < 0.05$). Effects of heatwave on RGR of *G. lemaneiformis* (C) and *S. costatum* (D) based on GAMs analysis. Solid lines and shadows are predicted values with 95 % confidence intervals, and the significant differences between the heatwave treatment and the control are justified by the lack of intersections of 95 % confidence intervals and the x-axis.

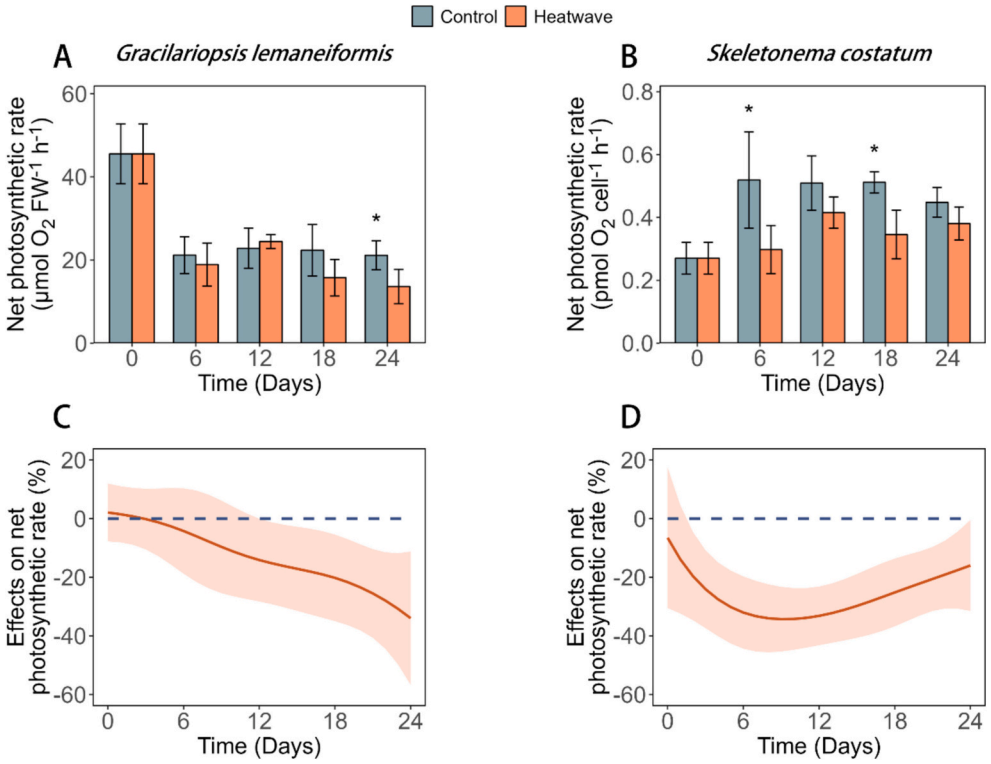

Fig. 3. The net photosynthetic rate of *G. lemaneiformis* (A) and *S. costatum* (B) under control and heatwave conditions. The value is mean ± standard deviation (SD), and * indicates that there is a significant difference between the control and the heatwave groups ($p < 0.05$). Effects of heatwave on net photosynthetic rate of *G. lemaneiformis* (C) and *S. costatum* (D) based on GAMs analysis. Solid lines and shadows are predicted values with 95 % confidence intervals, and the significant differences between the heatwave treatment and the control are justified by the lack of intersections of 95 % confidence intervals and the x-axis.

on *G. lemaneiformis* turned from positive to negative and the negative effect increased with culture time (Fig. 5C). Different from *G. lemaneiformis*, MHW did not impose significant effects on Chl *a* content in *S. costatum* during 24 days of culture (Fig. 5D). MHW did not affect carotenoids content in *G. lemaneiformis* or *S. costatum* at any time point (Fig. 6A&B). The effect patterns of MHW on carotenoids content in *G. lemaneiformis* and *S. costatum* were similar to those for Chl *a* content (Fig. 6C&D).

3.4. POC, PON content and C/N

Heatwave did not significantly affect POC content in *G. lemaneiformis* or *S. costatum* at any time point (ANOVA, $p > 0.05$, Fig. 7A& B). However, GAMs analysis showed that the responses of the two algae's POC content to the heatwave were different with time. During the heating phase, the POC content of *G. lemaneiformis* continued to be negatively affected, increasing from 2 % to 7 %, but the negative effect was alleviated during the heatwave maintenance phase, and gradually changed to a positive effect after the cooling period (Fig. 7C). Differently, the POC content of *S. costatum* was continuously negatively affected by the heatwave, which the highest inhibition rate reached about 20 %, and it was not relieved even during the recovery period (Fig. 7D). Heatwave did not significantly affect PON content in *G. lemaneiformis* or *S. costatum* at any time point, either (ANOVA, $p > 0.05$, Fig. 7E& F). The effects of heatwave on PON of both species showed a trend of continuous inhibition, but the degree of inhibition was different. The inhibition rate of heatwave on PON of *G. lemaneiformis* was less than 5 %, while that of *S. costatum* reached about 20 % (Fig. 7G&H).

In terms of C/N, heatwave did not affect it for *G. lemaneiformis* at any time point but increased it for *S. costatum* on day 24 (ANOVA, $p = 0.017$, Fig. 8A&B). The effect of heatwave on C/N in *G. lemaneiformis* varied from negative to positive with culture time while its effect on *S. costatum* was always positive and became larger with culture time (Fig. 8C&D).

3.5. Transcriptional response of G. lemaneiformis under MHW

After heatwave ended (D18) and heatwave recovered (D24), the transcriptome samples of *G. lemaneiformis* were sequenced and analyzed. The results showed that 59 DEGs were detected on the 18th day (end of the heatwave). Compared with the control group (17 °C BL), there were 39 (66 %) significantly up-regulated genes and 20 (34 %) significantly down-regulated genes in the heatwave group (20 °C HW) (Fig. 9A). On the 24th day (end of the recovery period), 116 DEGs were detected. Compared with the control group, there were 109 (94 %) significantly up-regulated genes and 7 (6 %) significantly down-regulated genes in the heatwave group (Fig. 9B).

In order to clarify the effect of heatwave treatment on the metabolic pathway of *G. lemaneiformis*, KEGG pathway enrichment analysis of DEGs was carried out. The analysis results showed that at the end of the heatwave (D18), the gene of 6-phosphofructokinase (*PFK*) involved in glycolysis pathway, a key enzyme for catalyzing fructose-6-phosphate to fructose-1,6-diphosphate, was significantly up-regulated by 5.67 $\log_2$ folds (Fig. 10A). However, the gene of pyruvate dehydrogenase complex (*PDHA*), which plays an important role in the conversion of pyruvate to Acetyl-CoA, was significantly down-regulated by 6.55 $\log_2$ folds. In addition, the gene of nitrate reductase (*NR*) that reduces nitrate to nitrite in nitrogen metabolism was up-regulated by 0.57 $\log_2$ folds (Fig. 10A).

After the recovery period of heatwave (D24), the genes of fatty acid acyl coenzyme hydratase (*echA*) and 3-hydroxy coenzyme A dehydrogenase (*HADH*) involved in fatty acid degradation pathway were both significantly up-regulated by 3.04 $\log_2$ folds, and phytoene dehydrogenase gene (*PSD*) in carotenoid biosynthesis pathway was significantly up-regulated by 1.13 $\log_2$ folds (Fig. 10B).

3.6. Transcriptional response of S. costatum under MHW

In order to analyze the molecular responses of *S. costatum* to MHW,

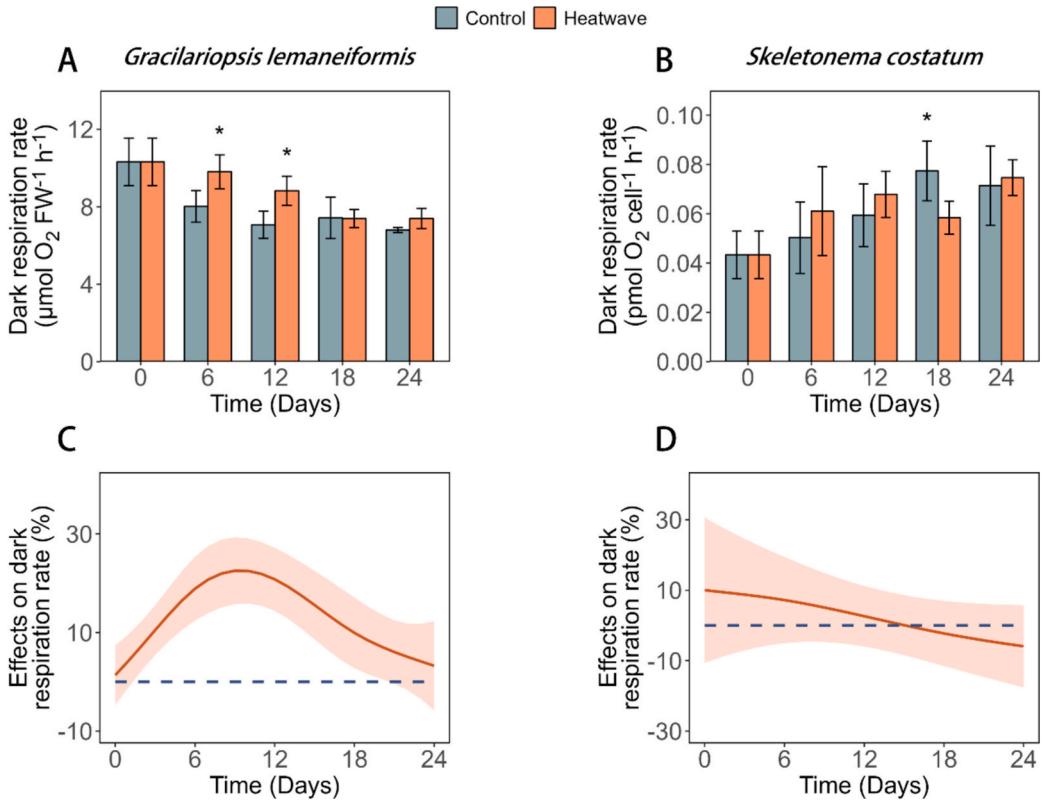

Fig. 4. The dark respiration rate of *G. lemaneiformis* (A) and *S. costatum* (B) under control and heatwave conditions. The value is mean ± standard deviation (SD), and * indicates that there is a significant difference between the control and the heatwave groups ($p < 0.05$). Effects of *G. lemaneiformis* (C) and *S. costatum* (D) heatwave group on dark respiration rate compared with control group. Solid lines and shadows are predicted values with 95 % confidence intervals by GAMs, and the significant differences between the heatwave treatment and the control are justified by the lack of intersections of 95 % confidence intervals and the x-axis.

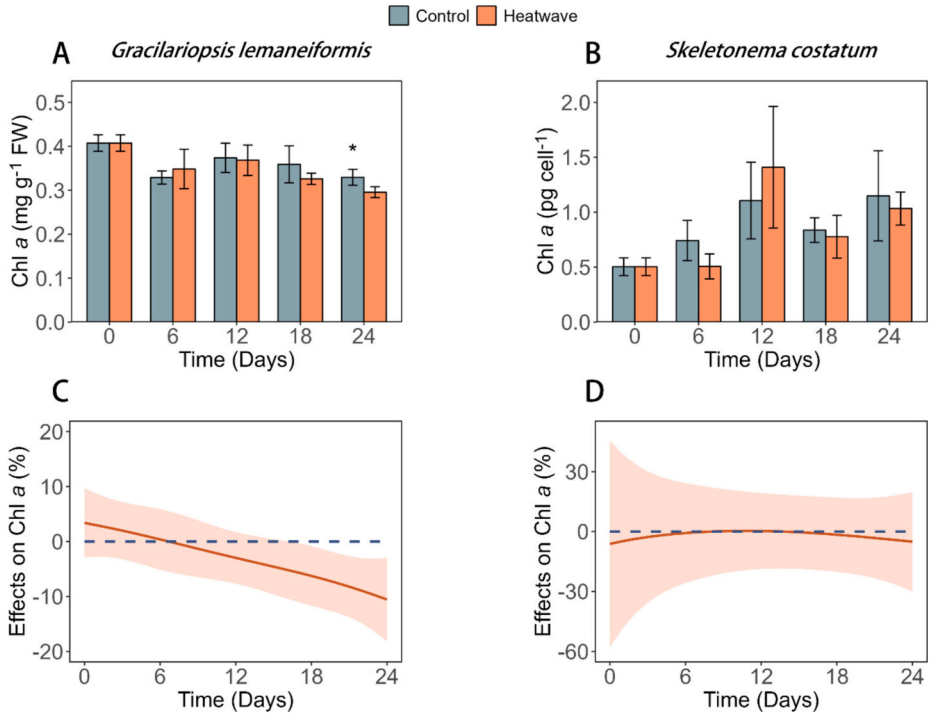

Fig. 5. The Chl *a* contents of *G. lemaneiformis* (A) and *S. costatum* (B) under control and heatwave conditions. The value is mean ± standard deviation (SD), and * indicates that there is a significant difference between the control and the heatwave groups ($p < 0.05$). Effects of heatwave on Chl *a* of *G. lemaneiformis* (C) and *S. costatum* (D) based on GAMs analysis. Solid lines and shadows are predicted values with 95 % confidence intervals, and the significant differences between the heatwave treatment and the control are justified by the lack of intersections of 95 % confidence intervals and the x-axis.

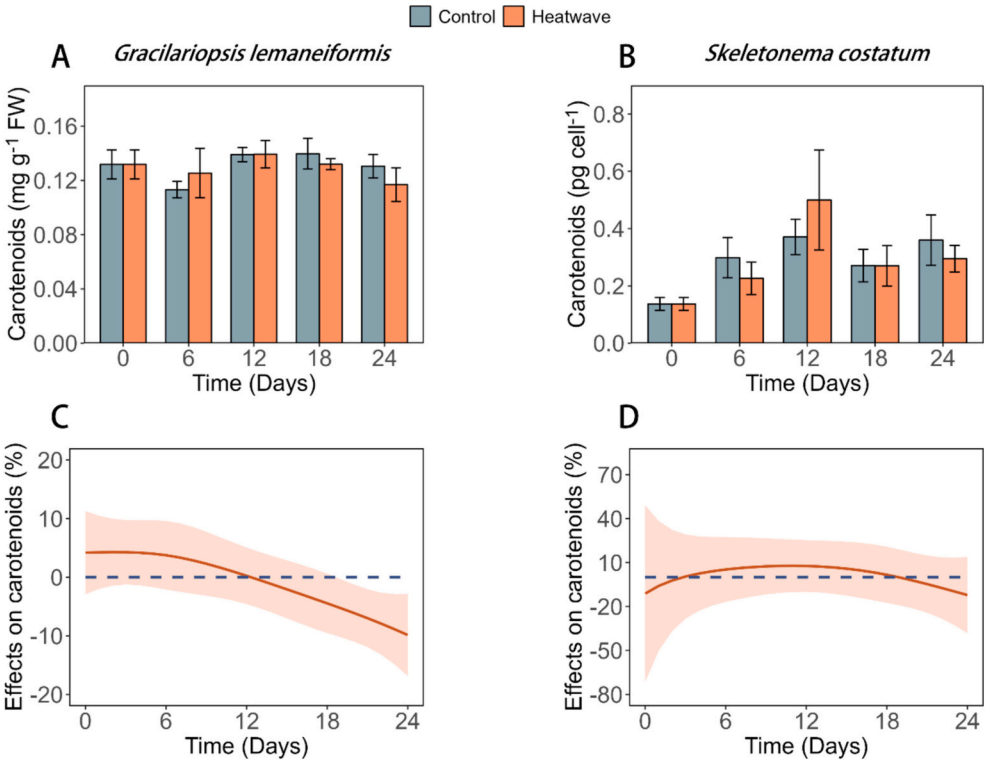

Fig. 6. The carotenoids contents of *G. lemaneiformis* (A) and *S. costatum* (B) under control and heatwave conditions. The value is mean ± standard deviation (SD), and * indicates that there is a significant difference between the control and the heatwave groups ($p < 0.05$). Effects of heatwave on carotenoids contents of *G. lemaneiformis* (C) and *S. costatum* (D) based on GAMs analysis. Solid lines and shadows are predicted values with 95 % confidence intervals, and the significant differences between the heatwave treatment and the control are justified by the lack of intersections of 95 % confidence intervals and the x-axis.

the gene expression of the control group and the heatwave group were compared. On the 18th day (at the end of the heatwave), a total of 3862 DEGs were detected. Compared with the control group (17 °C BL), there were 2665 (69 %) significantly up-regulated genes and 1197 (31 %) significantly down-regulated genes in *S. costatum* in the heatwave group (20 °C HW) (Fig. 11A). And on the 24th day (after the heatwave recovery period), 5498 DEGs were detected. Compared with the control group, *S. costatum* had 5240 (95 %) significantly up-regulated genes and 258 (5 %) significantly down-regulated genes (Fig. 11B).

On the 18th day, the enrichment results of KEGG pathway showed that the NADH dehydrogenase related genes (*Ndufs4*, *Ndufs7*, *Ndufs8*, *Ndufv1*, *Ndufv2*, *Ndufa6*, *Ndufa9*, *Ndufa12*) involved in oxidative phosphorylation biological oxidation process of *S. costatum* in heatwave group were significantly up-regulated by 4.41–6.45 $\log_2$ folds compared with the control group. At the same time, genes related to succinate dehydrogenase/fumarate reductase (*SDHC*, *SDHD*, *SDHA*) were significantly up-regulated by 5.56–7.25 $\log_2$ folds, genes related to cytochrome *c* reductase (*ISP*, *Cyt1*, *QCR7*) were significantly up-regulated by 3.58–7.39 $\log_2$ folds, and genes related to cytochrome *c* oxidase (*COX5B*, *COX6B*) were significantly up-regulated by 4.29 and 6.12 $\log_2$ folds, respectively. F-type ATPase-related genes (*alpha*, *beta*, *gamma*, *delta*, *OSCP*) were up-regulated by 0.54–7.08 $\log_2$ folds, while V-type ATPase-related genes (*A*, *B*, *E*, *H*, *a*, *c*, *d*) were significantly up-regulated by 0.58–5.58 $\log_2$ folds (Fig. 12A). The related genes of phosphoribokinase (*PRK*) and fructose diphosphate aldolase (*ALDO*) involved in Calvin cycle were up-regulated by 0.33–0.37 $\log_2$ folds, but the related genes of Sedoheptulose-1,7-bisphosphate (*glX-SEBP*) and ribulose-diphosphate carboxylase chain (*rbcL*) were down-regulated by 0.87 and 1.24 $\log_2$ folds, respectively (Fig. 12B). In addition, the genes related to key enzymes in glycolysis pathway, such as glucose phosphate isomerase (*PGI*), fructose-6-phosphate kinase (*PFK*), aldolase (*ALDO*), phosphoglycerate mutase (*PGAM*), enolase (*ENO*) and pyruvate kinase (*PK*), were up-regulated by 0.50–6.89 $\log_2$ folds. The related genes of most enzymes (*gltA*, *IDH2*, *OGDH*, *LSC1*, *SDHA*, *FH*) in TCA cycle pathway were significantly up-regulated by 3.88–8.14 $\log_2$ folds. In the meantime, most enzymes (*fadD*, *ACADM*, *HADH*) in fatty acid degradation pathway were also up-regulated. In nitrogen metabolism, the genes related to glutamine synthetase (*GLUL*) which converted ammonia into L-glutamine are significantly up-regulated by 5.50 $\log_2$ folds, while those related to glutamate synthetase (*GLU*) which subsequently converted L-glutamine into L-glutamate acid were significantly down-regulated by 2.00 $\log_2$ folds (Fig. 12C).

On the 24th day (after the recovery period of heatwave), compared with the control group, most enzymes related to glycolysis, TCA cycle, fatty acid degradation, Calvin cycle and nitrogen metabolism pathway were significantly up-regulated. The genes related to NADH dehydrogenase (*Ndufs1*, *Ndufs4*, *Ndufs7*, *Ndufv8*, *Ndufv1*, *Ndufv2*, *Ndufa2*, *Ndufa5*, *Ndufa9*, *Ndufab1*, *Ndufa12*, *Ndufb7*, *Ndufb9*) involved in oxidative phosphorylation were significantly up-regulated by 6.29–8.20 $\log_2$ folds. Genes related to succinate dehydrogenase/fumarate reductase (*SDHC*, *SDHD*, *SDHA*, *SDHB*, *SdhA*) were significantly up-regulated by 7.63–9.01 $\log_2$ folds, genes related to cytochrome *c* reductase (*ISP*, *Cyt1*, *QCR6*, *QCR7*) were significantly up-regulated by 5.18–8.65 $\log_2$ folds, genes related to cytochrome *c* oxidase (*COX5B*, *COX6B*) were significantly up-regulated by 7.05–7.53 $\log_2$ folds, and genes related to cytochrome *c* (*CYC*) was significantly up-regulated by 8.64 $\log_2$ folds. F-type ATPase-related genes (*beta*, *gamma*, *delta*, *OSCP*) were significantly up-regulated by 7.28–9.37 $\log_2$ folds, and V-type ATPase-related genes (*A*, *B*, *C*, *D*, *E*, *F*, *G*, *H*, *a*, *c*) were significantly up-regulated by 5.31–7.83 $\log_2$ folds (Fig. 13A). The enzymes related to Calvin cycle (*rpiA*, *PGK*, *GAPDH*, *ALDO*, *FBP*, *tktA*, *glx-SEBP*) were significantly up-regulated by 5.31–8.29 $\log_2$ folds (Fig. 13B). Furthermore, the related genes of various enzymes involved in glycolysis (*PGI*, *PFK*, *ALDO*, *GAPDH*, *PGK*, *PGAM*, *ENO*, *PK*) were significantly up-regulated by 5.47–8.29 $\log_2$ folds, and various enzymes involved in TCA cycle (*gltA*, *ACO*, *IDH2*, *OGDH*, *LSC1*, *SDHA*, *FH*, *MDH2*) were significantly up-regulated by

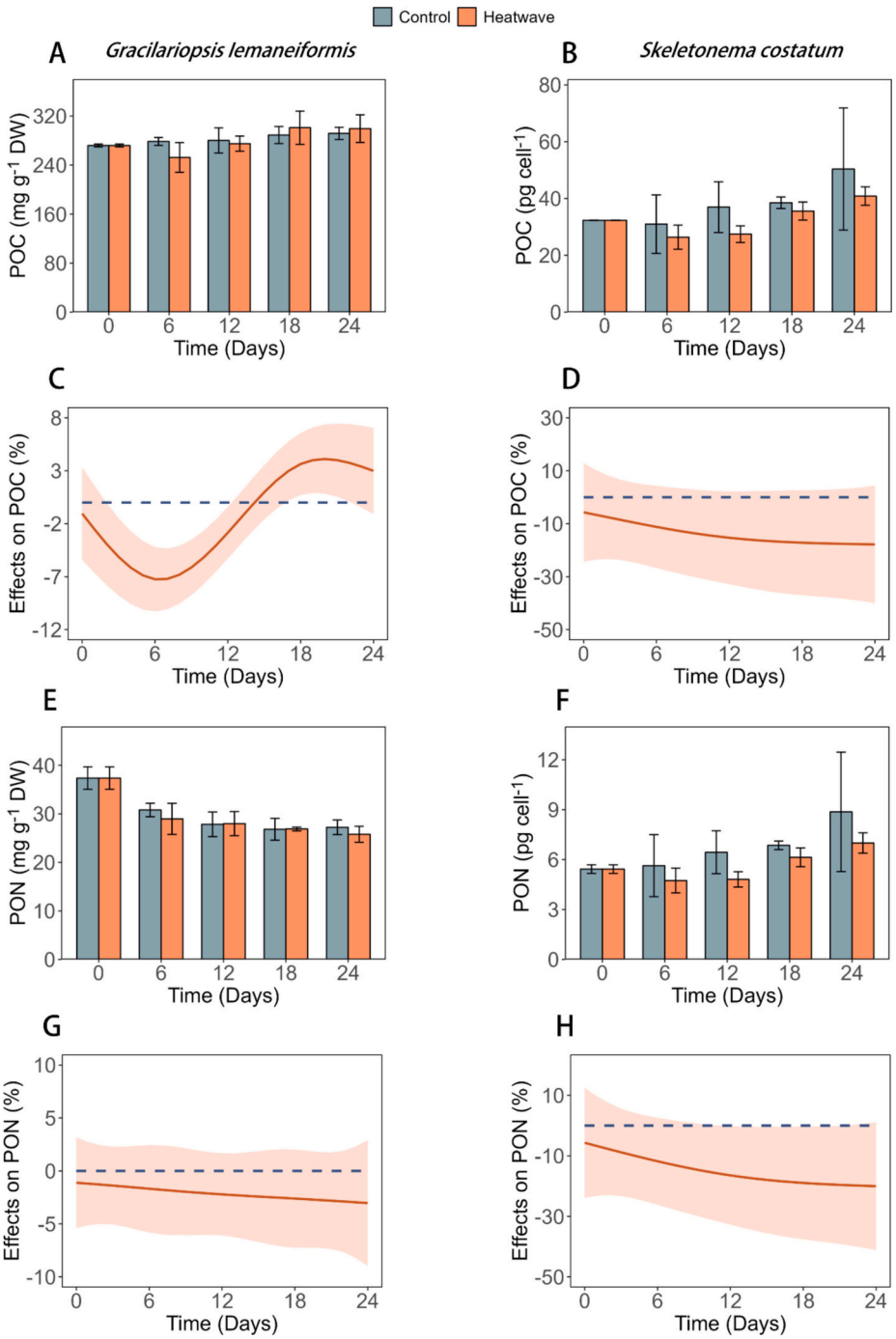

Fig. 7. The POC and PON contents of *G. lemaneiformis* (A, E) and *S. costatum* (B, F) under control and heatwave conditions. The value is mean ± standard deviation (SD), and * indicates that there is a significant difference between the control and the heatwave groups ($p < 0.05$). Effects of heatwave on POC and PON contents of *G. lemaneiformis* (C, G) and *S. costatum* (D, H) based on GAMs analysis. Solid lines and shadows are predicted values with 95 % confidence intervals, and the significant differences between the heatwave treatment and the control are justified by the lack of intersections of 95 % confidence intervals and the x-axis.

7.18–9.01 $\log_2$ folds. Genes of related enzymes (*fadD*, *ACADM*, *echA*, *HADH*) involved in fatty acid degradation pathway were significantly up-regulated by 6.25–8.49 $\log_2$ folds, and genes of related enzymes (*NR*, *GLUL*, *GLU*) were also significantly up-regulated in nitrogen metabolism (Fig. 13C).

4. Discussion

4.1. Physiological responses of G. lemaneiformis and S. costatum to MHW

In this study, the heatwave with a temperature increase of 3 °C from the baseline temperature of 17 °C caused damages to *G. lemaneiformis*. The negative effects of MHW on RGR of *G. lemaneiformis* increased with time. The previous study also showed that a 3 °C heatwave with the baseline temperature of 20 °C severely inhibited the growth of

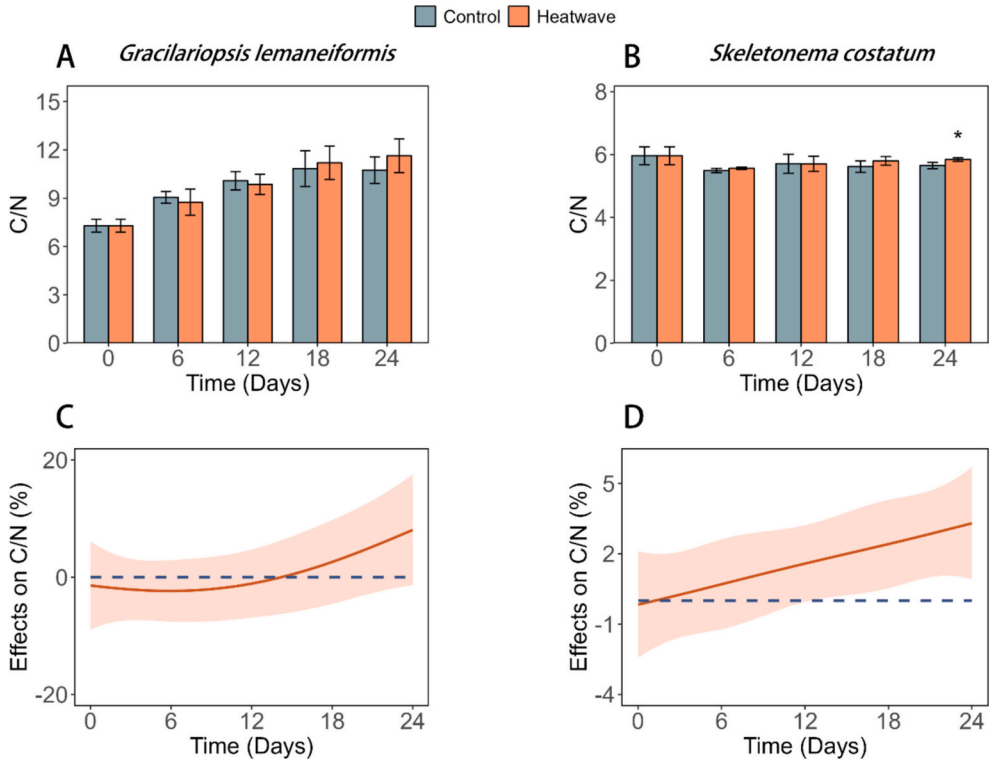

Fig. 8. The C/N of *G. lemaneiformis* (A) and *S. costatum* (B) under control and heatwave conditions. The value is mean ± standard deviation (SD), and * indicates that there is a significant difference between the control and the heatwave group ($p < 0.05$). Effects of heatwave on C/N of *G. lemaneiformis* (C) and *S. costatum* (D) based on GAMs analysis. Solid lines and shadows are predicted values with 95 % confidence intervals, and the significant differences between the heatwave treatment and the control are justified by the lack of intersections of 95 % confidence intervals and the x-axis.

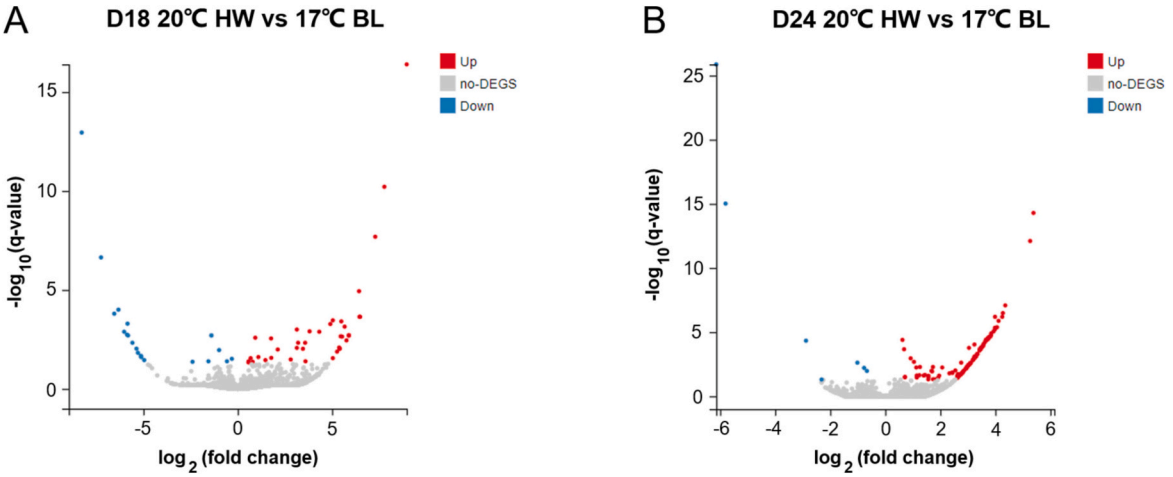

Fig. 9. Volcano plot of the DEGs in *G. lemaneiformis* between the heatwave and control groups on days 18 (A, at the end of heatwave) and 24 (B, after heatwave recovery). The red and blue dots indicate significantly up-regulated and down-regulated genes, respectively. (For interpretation of the references to colour in this figure legend, the reader is referred to the web version of this article.)

G. lemaneiformis (Jiang et al., 2022). Moreover, the partial bleaching of *G. lemaneiformis* showed that the drastic change of temperature during heatwave would cause sublethal pressure on *G. lemaneiformis* (Straub et al., 2019; Jiang et al., 2022). The negative effects of MHW on growth of *G. lemaneiformis* could be attributed to photosynthesis. The negative effects of MHW on net photosynthetic rate of *G. lemaneiformis* also increased with time, indicating that photosynthetic activity was significantly reduced even after a one-week recovery period. The inhibition of MHW on net photosynthetic rate was supported by reduced photosynthetic pigment, e.g., Chl *a*. Different from the physiological parameters mentioned above, MHW stimulated dark respiration rate of *G. lemaneiformis*, particularly during heatwave maintenance period. Increased dark respiration rate represents stronger metabolic activity that can benefit growth (Geider and Osborne, 1989). On the other hand, it is also a sign of cells dealing with environmental stress (Gao et al., 2017). In this study, relative growth rate was not enhanced under MHW and therefore the energy from increased dark respiration rate was used to confront thermal stress rather than for growth.

Previous studies have showed that the optimal growth temperature for *S. costatum* is around 25 °C and the increase from 17 to 20 °C should

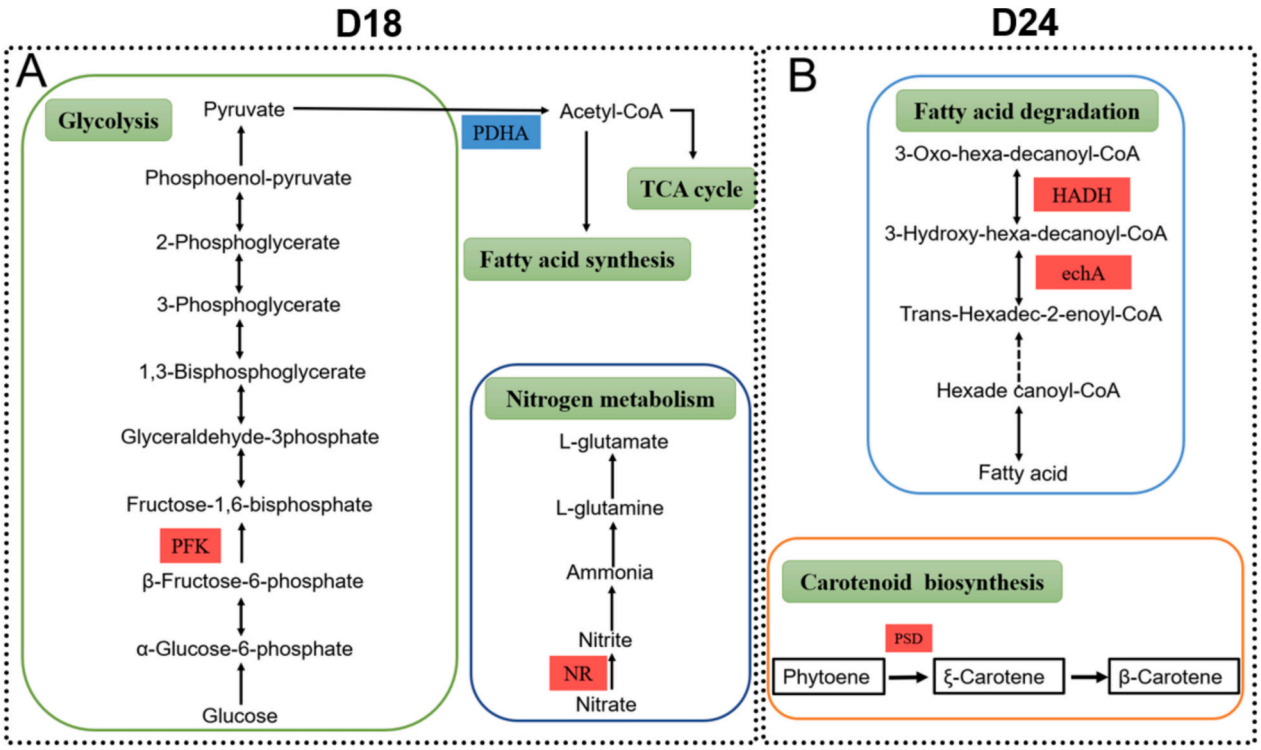

Fig. 10. KEGG pathways of *G. lemaneiformis* on day 18 (A, at the end of heatwave) and day 24 (B, after heatwave recovery). The red and blue indicate significantly up-regulated and down-regulated genes, respectively. (A) Gene expression of various enzymes in glycolysis, fatty acid degradation and nitrogen metabolism on the 18th day. (B) Gene expression of various enzymes in fatty acid degradation and carotenoid biosynthesis on the 24th day. (For interpretation of the references to colour in this figure legend, the reader is referred to the web version of this article.)

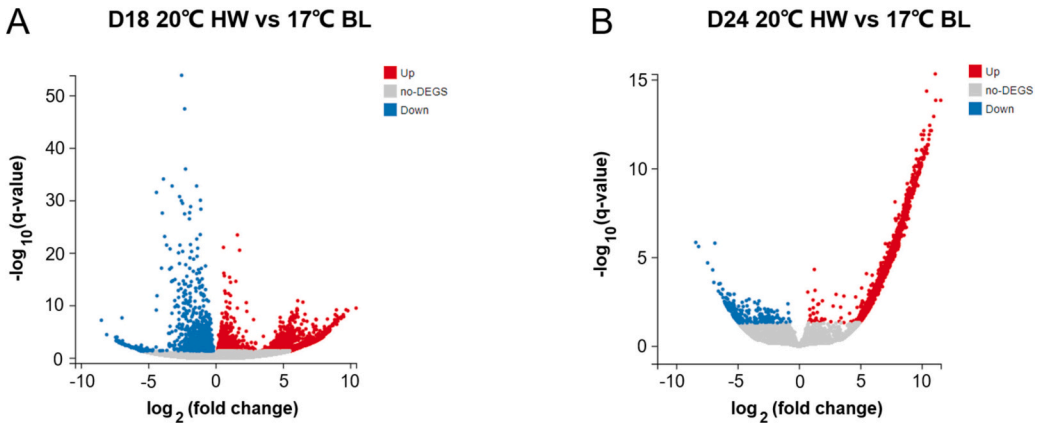

Fig. 11. Volcano plot of differentially expressed genes in *S. costatum* between the heatwave and control groups on days 18 (A, at the end of heatwave) and 24 (B, after heatwave recovery), with the red and blue dots indicating significantly up-regulated and down-regulated genes, respectively. (For interpretation of the references to colour in this figure legend, the reader is referred to the web version of this article.)

stimulate growth of *S. costatum* (Yan et al., 2002; Kaeriyama et al., 2011). However, the MHW (from 17 to 20 °C) in this study did not significantly increase growth of *S. costatum* and it even reduced relative growth rate of *S. costatum* on day 15. This is supported by the performance of net photosynthetic rate that was significantly reduced by MHW on days 6 and 18. We therefore presume that the inhibitions on growth and photosynthesis were from allelopathy of *G. lemaneiformis* rather than thermal stress since a 3 °C increase from 17 to 20 °C should be harmful for *S. costatum.* Our previous study also demonstrates that MHW could lead to the synthesis and release of allelochemicals in *G. lemaneiformis* (Gao et al., 2024). Allelochemicals from *G. lemaneiformis* can damage photosynthetic apparatus and activity of *S. costatum* (Gao et al., 2024). Dark respiration rate of *S. costatum* also decreased in heatwave group compared the control, indicating that allelochemicals from *G. lemaneiformis* could also negatively affect respiration related metabolic processes (e.g., glycolysis and TCA cycle).

4.2. Molecular responses of *G. lemaneiformis* and *S. costatum* to MHW

For *G. lemaneiformis*, at the end of the heatwave (D18), the *PFK* in glycolytic pathway of *G. lemaneiformis* was significantly increased, indicating that *G. lemaneiformis* may generate more energy to resist the stress of heatwave by accelerating glycolysis in response to heatwave. After one-week recovery from heatwave (D24), the transcriptome results showed that the degradation pathway of fatty acids was promoted, which indicates the influence of heatwave continued even after

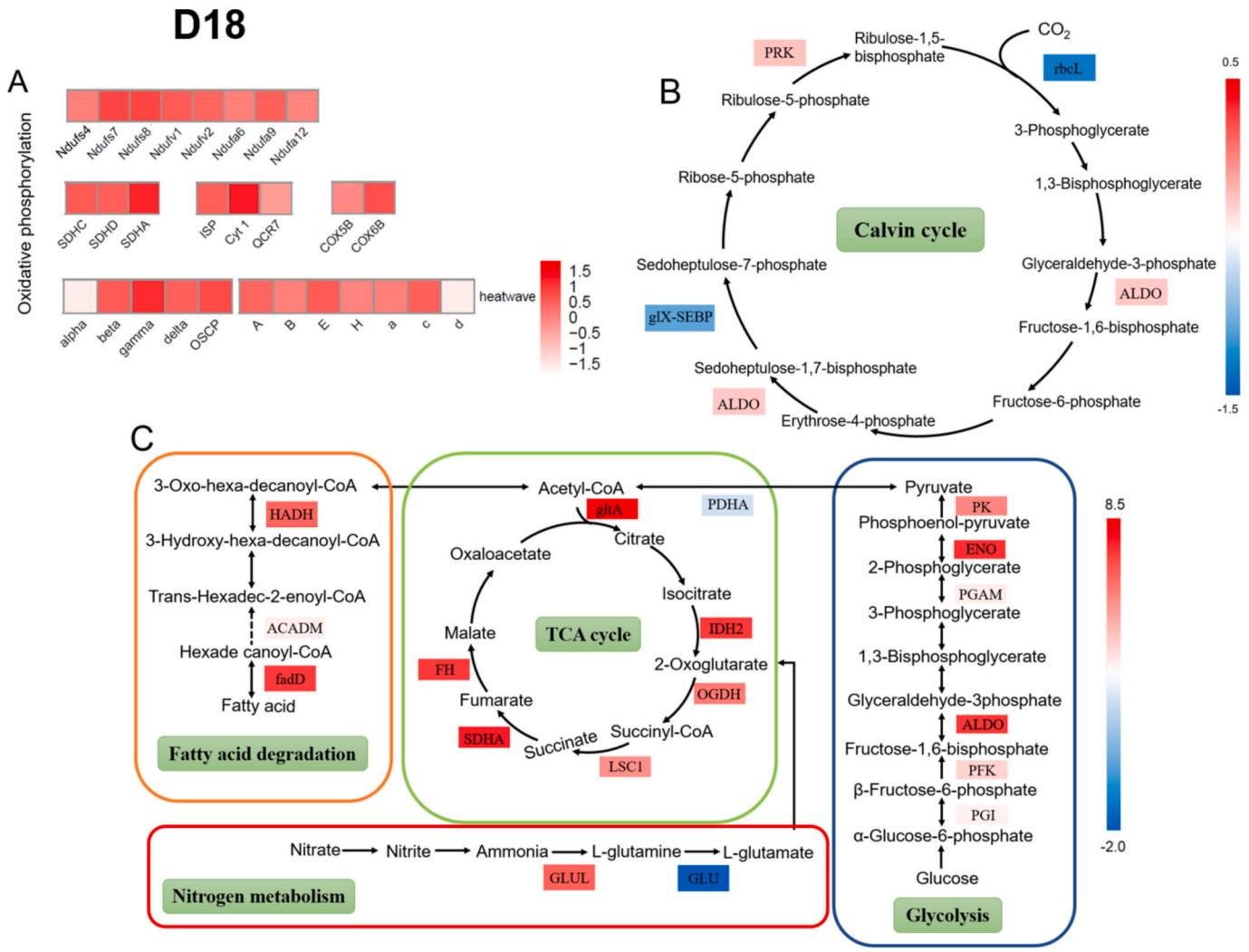

Fig. 12. KEGG pathways of *S. costatum* in the heatwave group on the 18th day (at the end of the heatwave), in which the colour represents the difference in $\log_2$ (fold change). (A) Heatmap of genes related to oxidative phosphorylation. (B) Gene expression of various enzymes in Calvin cycle. (C) Gene expression of various enzymes in glycolysis, TCA cycle, fatty acid degradation and nitrogen metabolism.

heatwave had ended. In addition, the change of temperature would affect the photosynthesis and respiration of algae, thus inducing the production of reactive oxygen species (ROS) (Graiff and Karsten, 2021), which would activate the antioxidant defense mechanism of algae to reduce the oxidative damage of algae (Lesser, 2006). But when the formation of ROS exceeded the antioxidant defense ability of organisms, such as the drastic temperature change caused by heatwave, it may lead to oxidative damage of protein and DNA. On the 24th day, the transcriptome results showed that β-carotene with antioxidant activity (Bai et al., 2005) was significantly up-regulated in its synthesis pathway (Fig. 10B), indicating that *G. lemaneiformis* actively responded to MHW stress. However, the carotenoid content of *G. lemaneiformis* in heatwave group was still slightly lower than that in control group, which may indicate that the detrimental effects of MHW had exceeded the capability of *G. lemaneiformis* to repair oxidative damage and thus destroyed the redox balance of cells, leading to the decrease of its RGR (Geigenberger and Fernie, 2014). It was verified by the physiological results of the continuous decrease of its RGR.

By contrast, at the end of heatwave, many enzymes related to oxidative phosphorylation pathway in *S. costatum* were significantly up-regulated (Fig. 12A), indicating that *S. costatum* strengthened energy metabolism to deal with the stress of MHW. Signal pathway mediated by ROS affected the transcription and translation of genes and regulated carbon metabolism and energy metabolism pathway of algae to resist oxidative damage (Zhang et al., 2022). The TCA cycle was a symbolic energy generation pathway, which was responsible for oxidizing respiratory substrates to drive ATP synthesis (Sweetlove et al., 2010). Transcriptome results showed that most enzymes related to oxidative phosphorylation, glycolysis and TCA cycle were significantly up-regulated (Fig. 12A&C). It indicates that *S. costatum* could cope with the stress of MHW and *G. lemaneiformis* through various energy metabolism pathways, so the accumulation of POC and PON in cells was reduced, which was also consistent with the measured physiological results. The contents of POC and PON in *S. costatum* in heatwave group were slightly lower than those in control group (Fig. 7B&F). At the same time, *rbcL* and *glX-SEBP* in Calvin cycle was significantly decreased when the heatwave ended (D18) (Fig. 12B), which supports the decreased net photosynthetic rate. It seems that *S. costatum* did not address the stress from MHW and *G. lemaneiformis* by the end of heatwave, indicated by net photosynthetic rate and relative growth rate, although it enhanced its responses in oxidative phosphorylation, glycolysis and TCA cycles.

After the recovery period of heatwave, more enzymes related to oxidative phosphorylation, glycolysis and fatty acid degradation in *S. costatum* were significantly increased (Fig. 13), which accelerated the energy flow and improved its own nitrogen metabolism pathway. Previous studies had shown that plants could improve the biosynthesis of

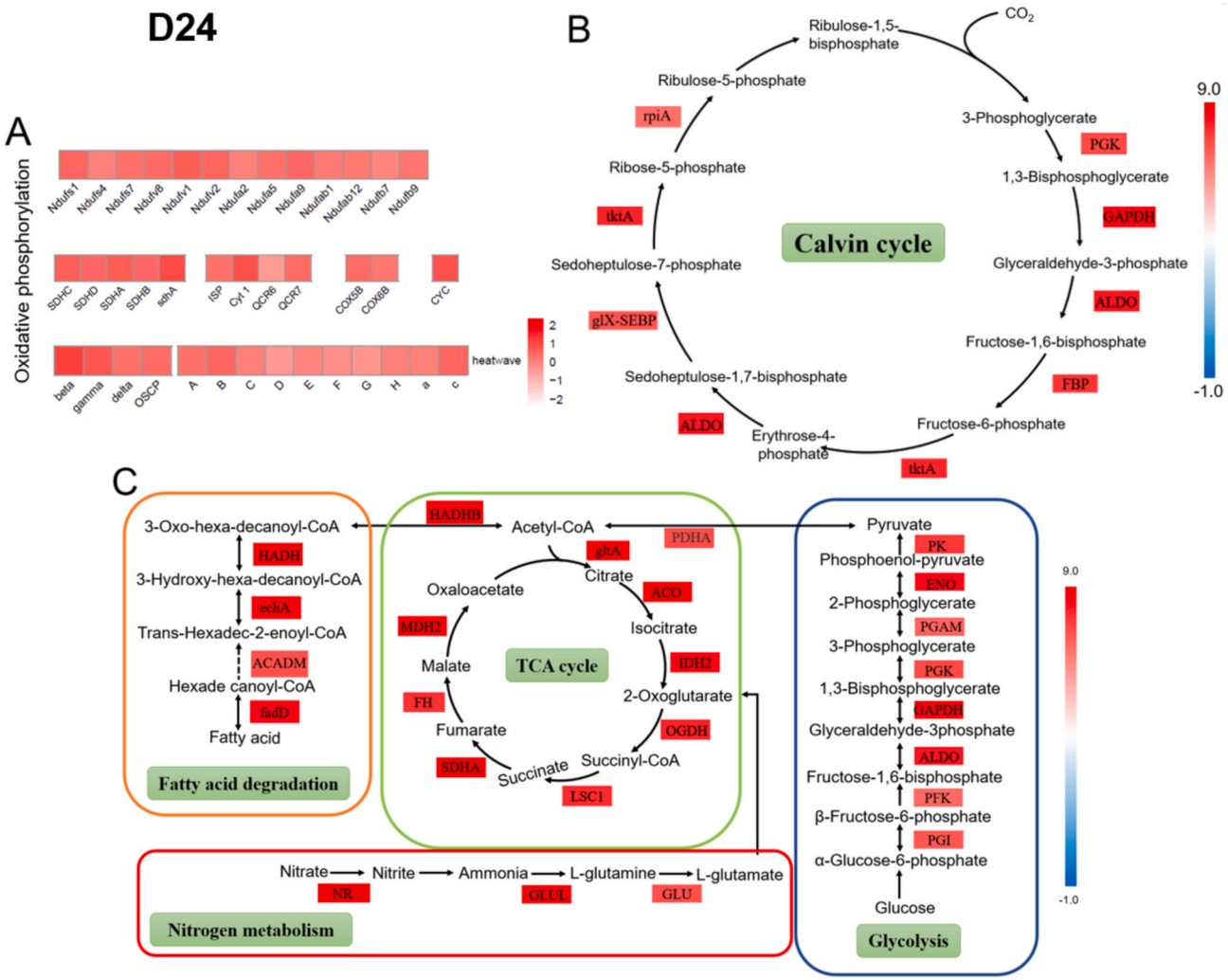

Fig. 13. KEGG pathways of *S. costatum* in heatwave group on the 24th day (after heatwave recovery), in which the colour represents the difference in $\log_2$ (fold change). (A) Heatmap of genes related to oxidative phosphorylation. (B) Gene expression of various enzymes in Calvin cycle. (C) Gene expression of various enzymes in glycolysis, TCA cycle, fatty acid degradation and nitrogen metabolism.

nitrogen-containing compounds such as amino acids, protein and nucleic acids to stabilize the cell morphology and protein structure, promote the synthesis of chlorophyll, strengthen photosynthesis (Alipanah et al., 2015), and reduce the production of ROS in the cell to affect the ability of plants to resist environmental stress (Khoshbakht et al., 2018). The significant up-regulation of *NR*, *GLUL* and *GLU* related genes in nitrogen metabolism pathway of *S. costatum* indicated that it had strong resistance to MHW stress and self-repair ability. At the same time, most enzymes in Calvin cycle pathway were significantly up-regulated (Fig. 13B), indicating that *S. costatum* used ATP produced by TCA cycle and other ways to improve its photosynthetic carbon fixation, so as to repair the damage caused by MHW and *G. lemaneiformis*. Due to more up-regulated genes compare to those at the end of heatwave, the net photosynthetic rate and dark respiration rate of *S. costatum* were completely repaired by the end of heatwave recovery period. Consequently, the relative growth rate was even higher under MHW treatment.

4.3. Differential responses of two algae to MHW and potential implications

Physiological responses of *G. lemaneiformis* and *S. costatum* to MHW were different. The negative effect of MHW on relative growth rate of *G. lemaneiformis* increased with culture time even after a one-week recovery period. On the other hand, the negative effect of MHW on relative growth rate of *S. costatum* was smaller than *G. lemaneiformis* and relative growth rate of *S. costatum* was even higher under MHW treatment compared to control after a one-week recovery period. Similar to relative growth rate, net photosynthetic rate of *G. lemaneiformis* was lower under MHW treatment even by the end of recovery period while there was no significant difference between MHW and control groups for *S. costatum*. A similar trend also occurred in Chl *a* content. In addition to physiological performances, *G. lemaneiformis* and *S. costatum* also showed differential molecular responses to MHW. The numbers of DEGs in *G. lemaneiformis* were 59 and 116 on the 18th and 24th days respectively. Only several genes involved in fatty acid degradation, glycolysis and carotenoid biosyenhtesis were up-regulated, indicating that the self-regulation ability of *G. lemaneiformis* to acclimate to the heatwave was weak. By contrast, the numbers of DEGs in *S. costatum* reached 3862 and 5498 on the 18th and 24th days respectively. A multitude of genes involved in oxidative phosphorylation, glycolysis, TCA cycle, fatty acid degradation, Calvin cycle and nitrogen metabolism were significantly up-regulated. This robust response signifies that *S. costatum* possesses a formidable capacity for self-regulation and repair, enabling it to effectively manage and acclimate to environmental stressors.

Combing physiological and molecular responses, *S. costatum* showed a stronger capacity to deal with MHW compared to *G. lemaneiformis*.

Therefore, *S. costatum* may gain competitive advantages against *G. lemaneiformis* in future MHW scenarios. In seaweed cultivation areas, there is usually no HABs due to the inhibition of high-density seaweed biomass (Yang et al., 2015; Gao et al., 2019). The findings in this study indicate that the competition advantages may shift from seaweed to bloom-forming algae, leading to the occurrence of HABs in seaweed cultivation areas in MHW increasing future. Intense HABs can rapidly exhaust essential nutrients including DIN and DIP in cultivation seawater and diminish the light intensity accessible to seaweeds, thereby inhibiting growth of seaweeds. Therefore, the direct negative effects of MHWs on growth of *G. lemaneiformis* combined with increased competition from bloom-forming microalgae, are likely to result in substantial consequences. This will ultimately lead to losses of seaweed production and associated industries, e.g., abalone culture and agar processing, impairing local economy. The limited transcriptional responses in *G. lemaneiformis* to MHWs are prone to induce the declines in the net photosynthetic rate and an elevation in the dark respiration rate. Such alterations can subsequently give rise to a reduction in carbon fixation and sequestration by seaweed cultivation. Moreover, it will also undermine the capacity of seaweed cultivation to alleviate ocean acidification and deoxygenation, thereby diminishing its positive ecological role in these aspects (Xiao et al., 2021; Gao et al., 2022). In the face of the potential losses in seaweed cultivation caused by MHWs, the development of heat-resistant strains or species is of utmost importance for the future. Sustainable seaweed cultivation and its scale expansion will be crucial in reducing and preventing the occurrence of red tides. In addition, the modified clay method is considered as an effective emergency treatment technology for red tides (Yu et al., 2023) and it can be employed in seaweed cultivation areas to reduce the competitive advantage of bloom-forming microalgae under MHW conditions. Meanwhile, strict measures for greenhouse gas emission reduction and removal must be implemented to mitigate climate change and extreme weather.

5. Conclusion

Marine heatwaves (MHWs) are occurring with increasing frequency and severity due mainly to global warming. Despite this, the competition dynamics between cultivated seaweeds and bloom-forming microalgae under MHW remains unclear. This study carried out a coculture of *G. lemaneiformis* and *S. costatum* under a simulated MHW to address this knowledge gap. Under the simulated heatwave, physiological parameters such as relative growth rate, net photosynthetic rate and photosynthetic pigment of the macroalga *G. lemaneiformis* were continuously reduced, and did not recover even after a one-week recovery period. However, by modulating its energy metabolism and upregulating the expression of relevant genes, *S. costatum* could deal well with MHW and competition stress, gaining competitive edge over *G. lemaneiformis*. Consequently, under the projected stress of extreme weather events in the future, the inhibition of *G. lemaneiformis* on *S. costatum* may diminish, potentially escalating the risk of HABs in seaweed cultivation areas. However, it is uncertain whether these responses can be generalized to other macroalgae and bloom-forming microalgae. To further elucidate the impacts of MHWs on algal competition and community structure, forthcoming research should encompass a broader range of algal species. This should involve not only cultivated species such as *Saccharina* and *Pyropia* but also bloom-forming cyanobacteria and dinoflagellates. Furthermore, investigations should be extended to include the seasonal impacts of MHWs and the synergistic effects of MHWs in combination with other environmental elements, such as nutrients and light.

CRediT authorship contribution statement

Xin Zhao: Writing – review & editing, Writing – original draft, Visualization, Methodology, Formal analysis. **Lin Gao:** Writing – review & editing, Writing – original draft, Visualization, Methodology, Investigation, Formal analysis, Data curation. **Xu Li:** Writing – review & editing, Methodology. **Gang Li:** Writing – review & editing, Resources, Funding acquisition. **Guang Gao:** Writing – review & editing, Writing – original draft, Supervision, Resources, Methodology, Funding acquisition, Formal analysis, Conceptualization.

Declaration of competing interest

The authors declare that they have no known competing financial interests or personal relationships that could have appeared to influence the work reported in this paper.

Data availability

Data will be made available on request.

Acknowledgments

This work was supported by the National Natural Science Foundation of China (42076154), the Natural Science Foundation of Fujian Province (2022J01026, 2021J01026), Xiamen University Pingtan Institute (XMUPTI2024001), and the MEL Internal Research Program (MELRI2304). The authors also appreciate the support from Google Climate Action Research Awards, and the laboratory technicians Wenyan Zhao and Xianglan Zeng.

Appendix A. Supplementary data

Supplementary data to this article can be found online at https://doi.org/10.1016/j.aquaculture.2024.742111.

References

Alipanah, L., Rohloff, J., Winge, P., Bones, A.M., Brembu, T., 2015. Whole-cell response to nitrogen deprivation in the diatom *Phaeodactylum tricornutum*. J. Exp. Bot. 66, 6281–6296. https://doi.org/10.1093/jxb/erv340.

Anderson, D.M., Fensin, E., Gobler, C.J., Hoeglund, A.E., Hubbard, K.A., Kulis, D.M., Landsberg, J.H., Lefebvre, K.A., Provoost, P., Richlen, M.L., Smith, J.L., Solow, A.R., Trainer, V.L., 2021. Marine harmful algal blooms (HABs) in the United States: history, current status and future trends. Harmful Algae 102, 101975. https://doi.org/10.1016/j.hal.2021.101975.

Bai, S.K., Lee, S.J., Na, H.J., Ha, K.S., Han, J.A., Lee, H., Kwon, Y.G., Chung, C.K., Kim, Y. M., 2005. β-carotene inhibits inflammatory gene expression in lipopolysaccharide-stimulated macrophages by suppressing redox-based NF-κB activation. Exp. Mol. Med. 37, 323–334. https://doi.org/10.1038/emm.2005.42.

Chai, Z.Y., He, Z.L., Deng, Y.Y., Yang, Y.F., Tang, Y.Z., 2018. Cultivation of seaweed *Gracilaria lemaneiformis* enhanced biodiversity in a eukaryotic plankton community as revealed via metagenomic analyses. Mol. Ecol. 27, 1081–1093. https://doi.org/10.1111/mec.14496.

Donovan, M.K., Burkepile, D.E., Kratochwill, C., Shlesinger, T., Sully, S., Oliver, T.A., Hodgson, G., Freiwald, J., van Woesik, R., 2021. Local conditions magnify coral loss after marine heatwaves. Science 372, 977–980. https://doi.org/10.1126/science.abd9464.

Du, X., Peterson, W.T., 2018. Phytoplankton community structure in 2011–2013 compared to the extratropical warming event of 2014–2015. Geophys. Res. Lett. 45, 1534–1540. https://doi.org/10.1002/2017GL076199.

Fei, X., 2004. Solving the coastal eutrophication problem by large scale seaweed cultivation. Hydrobiologia 512, 145–151. https://doi.org/10.1023/B:HYDR.0000020320.68331.ce.

Feng, Y., Xiong, Y., Hall-Spencer, J.M., Liu, K., Beardall, J., Gao, K., Ge, J., Xu, J., Gao, G., 2024. Shift in algal blooms from micro- to macroalgae around China with increasing eutrophication and climate change. Glob. Chang. Biol. 30, 1–16. https://doi.org/10.1111/gcb.17018.

Fischer, A.D., Houliez, E., Bill, B.D., Kavanaugh, M.T., Alin, S.R., Collins, A.U., Kudela, R. M., Moore, S.K., 2024. Nutrient limitation dampens the response of a harmful algae to a marine heatwave in an upwelling system. Limnol. Oceanogr. https://doi.org/10.1002/lno.12604.

Gao, G., Liu, Y., Li, X., Feng, Z., Xu, Z., Wu, H., Xu, J., 2017. Expected CO_2-induced ocean acidification modulates copper toxicity in the green tide alga *Ulva prolifera*. Environ. Exp. Bot. 135, 63–72. https://doi.org/10.1016/j.envexpbot.2016.12.007.

Gao, G., Fu, Q., Beardall, J., Wu, M., Xu, J., 2019. Combination of ocean acidification and warming enhances the competitive advantage of *Skeletonema costatum* over a green tide alga, *Ulva linza*. Harmful Algae 85, 101698. https://doi.org/10.1016/j.hal.2019.101698.

Gao, G., Gao, L., Jiang, M., Jian, A., He, L., 2022. The potential of seaweed cultivation to achieve carbon neutrality and mitigate deoxygenation and eutrophication. Environ. Res. Lett. 17, 014018. https://doi.org/10.1088/1748-9326/ac3fd9.

Gao, L., Xiong, Y., Fu, F.X., Hutchins, D.A., Gao, K., Gao, G., 2024. Marine heatwaves alter competition between the cultured macroalga *Gracilariopsis lemaneiformis* and the harmful bloom alga *Skeletonema costatum*. Sci. Total Environ. 947, 174345. https://doi.org/10.1016/j.scitotenv.2024.174345.

Geider, R.J., Osborne, B.A., 1989. Respiration and microalgal growth: a review of the quantitative relationship between dark respiration and growth. New Phytol. 112, 327–341. https://doi.org/10.1111/j.1469-8137.1989.tb00321.x.

Geigenberger, P., Fernie, A.R., 2014. Metabolic control of redox and redox control of metabolism in plants. Antioxid. Redox Signal. 21, 1389–1421. https://doi.org/10.1089/ars.2014.6018.

Graiff, A., Karsten, U., 2021. Antioxidative properties of Baltic Sea keystone macroalgae (*Fucus vesiculosus*, phaeophyceae) under ocean warming and acidification in a seasonally varying environment. Biology (Basel) 10, 1330. https://doi.org/10.3390/biology10121330.

Hayashida, H., Matear, R.J., Strutton, P.G., 2020. Background nutrient concentration determines phytoplankton bloom response to marine heatwaves. Glob. Chang. Biol. 26, 4800–4811. https://doi.org/10.1111/gcb.15255.

He, W., Zeng, X., Deng, L., Chun Pi, Q.L., Zhao, J., 2023. Enhanced impact of prolonged MHWs on satellite-observed chlorophyll in the South China Sea. Prog. Oceanogr. 218, 103123. https://doi.org/10.1016/j.pocean.2023.103123.

Jiang, M., Gao, L., Huang, R., Lin, X., Gao, G., 2022. Differential responses of bloom-forming *Ulva intestinalis* and economically important *Gracilariopsis lemaneiformis* to marine heatwaves under changing nitrate conditions. Sci. Total Environ. 840, 156591. https://doi.org/10.1016/j.scitotenv.2022.156591.

Jiang, M., Hall-Spencer, J.M., Gao, L., Ma, Z., Gao, G., 2024. Nitrogen availability regulates the effects of a simulated marine heatwave on carbon sequestration and phycosphere bacteria of a marine crop. Limnol. Oceanogr. 69, 339–354. https://doi.org/10.1002/lno.12487.

Kaeriyama, H., Katsuki, E., Otsubo, M., Yamada, M., Ichimi, K., Tada, K., Harrison, P.J., 2011. Effects of temperature and irradiance on growth of strains belonging to seven Skeletonema species isolated from Dokai Bay, southern Japan. Eur. J. Phycol. 46, 113–124. https://doi.org/10.1080/09670262.2011.565128.

Kelly, K.J., Mansour, A., Liang, C., Kim, A.M., Mancini, L.A., Bertin, M.J., Jenkins, B.D., Hutchins, D.A., Fu, F.X., 2023. Simulated upwelling and marine heatwave events promote similar growth rates but differential domoic acid toxicity in Pseudo-nitzschia australis. Harmful Algae 127, 102467. https://doi.org/10.1016/j.hal.2023.102467.

Khoshbakht, D., Asghari, M.R., Haghighi, M., 2018. Influence of foliar application of polyamines on growth, gas-exchange characteristics, and chlorophyll fluorescence in *Bakraii citrus* under saline conditions. Photosynthetica 56, 731–742. https://doi.org/10.1007/s11099-017-0723-2.

Kuroda, H., Setou, T., 2021. Extensive marine heatwaves at the sea surface in the northwestern pacific ocean in summer 2021. Remote Sens. 13, 3989. https://doi.org/10.3390/rs13193989.

Langmead, Ben, Salzberg, S.L., 2012. Fast gapped-read alignment with Bowtie 2. Nat. Methods 9, 357–360. https://doi.org/10.1038/nmeth.1923.

Laufkötter, C., Zscheischler, J., Frölicher, T.L., 2020. High-impact marine heatwaves attributable to human-induced global warming. Science 369, 1621–1625.

Lesser, M.P., 2006. Oxidative stress in marine environments: biochemistry and physiological ecology. Annu. Rev. Physiol. 68, 253–278. https://doi.org/10.1146/annurev.physiol.68.040104.110001.

Li, B., Dewey, C.N., 2011. RSEM: accurate transcript quantification from RNA-Seq data with or without a reference genome. BMC Bioinformatics 12, 1–16. https://doi.org/10.1186/1471-2105-12-323.

Li, Xiaodong, Su, L., Li, Xiaojie, Li, J., Xu, Y., Chang, L., Yu, R., Yang, D., Pang, S., 2022. Comprehensive analyses of large-scale *Saccharina japonica* damage in the principal farming area of Rongcheng Shandong Province in 2021-2022. J. Agric. Sci. Technol. https://doi.org/10.13304/j.nykjdb.2022.0728.

Oliver, E.C.J., Lago, V., Hobday, A.J., Holbrook, N.J., Ling, S.D., Mundy, C.N., 2018. Marine heatwaves off eastern Tasmania: trends, interannual variability, and predictability. Prog. Oceanogr. 161, 116–130. https://doi.org/10.1016/j.pocean.2018.02.007.

Pecl, G.T., Araújo, M.B., Bell, J.D., Blanchard, J., Bonebrake, T.C., Chen, I.C., Clark, T.D., Colwell, R.K., Danielsen, F., Evengård, B., Falconi, L., Ferrier, S., Frusher, S., Garcia, R.A., Griffis, R.B., Hobday, A.J., Janion-Scheepers, C., Jarzyna, M.A., Jennings, S., Lenoir, J., Linnetved, H.I., Martin, V.Y., McCormack, P.C., McDonald, J., Mitchell, N.J., Mustonen, T., Pandolfi, J.M., Pettorelli, N., Popova, E., Robinson, S.A., Scheffers, B.R., Shaw, J.D., Sorte, C.J.B., Strugnell, J.M., Sunday, J. M., Tuanmu, M.N., Vergés, A., Villanueva, C., Wernberg, T., Wapstra, E., Williams, S. E., 2017. Biodiversity redistribution under climate change: impacts on ecosystems and human well-being. Science 355, eaai9214. https://doi.org/10.1126/science.aai9214.

Porra, R.J., Thompson, W.A.A., Kriedemann, P.E., 1989. Determination of accurate extinction coefficients and simultaneous equations for assaying chlorophylls a and b extracted with four different solvents: verification of the concentration of chlorophyll standards by atomic absorption spectroscopy. Biochim. Biophys. Acta 975, 384–394.

Remy, M., Hillebrand, H., Flöder, S., 2017. Stability of marine phytoplankton communities facing stress related to global change: interactive effects of heat waves and turbidity. J. Exp. Mar. Biol. Ecol. 497, 219–229. https://doi.org/10.1016/j.jembe.2017.10.002.

Smith, K.E., Burrows, M.T., Hobday, A.J., King, N.G., Moore, P.J., Sen Gupta, A., Thomsen, M.S., Wernberg, T., Smale, D.A., 2023. Biological impacts of marine heatwaves. Annu. Rev. Mar. Sci. 15, 119–145. https://doi.org/10.1146/annurev-marine-032122-121437.

Straub, S.C., Wernberg, T., Thomsen, M.S., Moore, P.J., Burrows, M.T., Harvey, B.P., Smale, D.A., 2019. Resistance, extinction, and everything in between – the diverse responses of seaweeds to marine heatwaves. Front. Mar. Sci. 6, 763. https://doi.org/10.3389/fmars.2019.00763.

Strickland, J.D.H., Parsons, T.R., 1972. A Practical Handbook of Seawater Analysis. https://doi.org/10.2307/1979241.

Sweetlove, L.J., Beard, K.F.M., Nunes-Nesi, A., Fernie, A.R., Ratcliffe, R.G., 2010. Not just a circle: flux modes in the plant TCA cycle. Trends Plant Sci. 15, 462–470. https://doi.org/10.1016/j.tplants.2010.05.006.

Takagi, S., Kuroda, H., Hasegawa, N., Watanabe, T., Unuma, T., Taniuchi, Y., Yokota, T., Izumida, D., Nakagawa, T., Kurokawa, T., Azumaya, T., 2022. Controlling factors of large-scale harmful algal blooms with Karenia selliformis after record-breaking marine heatwaves. Front. Mar. Sci. 9, 1–14. https://doi.org/10.3389/fmars.2022.939393.

Wang, Z.L., Li, R.X., Zhu, M.Y., Chen, B.Z., Hao, Y.J., 2006. Study on population growth processes and interspecific competition of *Prorocentrum donghaiense* and *Skeletonema costatum* in semi-continuous dilution experiments. Adv. Mar. Sci. 24, 495–503. https://doi.org/10.3969/j.issn.1671-6647.2006.04.011.

Wells, M.L., Trainer, V.L., Smayda, T.J., Karlson, B.S.O., Trick, C.G., Kudela, R.M., Ishikawa, A., Bernard, S., Wulff, A., Anderson, D.M., Cochlan, W.P., 2015. Harmful algal blooms and climate change: learning from the past and present to forecast the future. Harmful Algae 49, 68–93. https://doi.org/10.1016/j.hal.2015.07.009.

Xiao, X., Agustí, S., Yu, Y., Huang, Y.Z., Chen, W.Z., Hu, J., Li, C., Li, K., Wei, F.Y., Lu, Y. T., Xu, C.C., Chen, Z.P., Liu, S.P., Zeng, J.N., Wu, J.P., Duarte, C.M., 2021. Seaweed farms provide refugia from ocean acidification. Sci. Total Environ. 776, 145192. https://doi.org/10.1016/j.scitotenv.2021.145192.

Yan, T., Zhou, M.J., Qian, P.Y., 2002. Combined effects of temperature, irradiance and salinity on growth of diatom *Skeletonema Costatum*. Chin. J. Oceanol. Limnol. 20, 237–243. https://doi.org/10.1007/BF02848852.

Yang, Y., Liu, Q., Chai, Z., Tang, Y., 2015. Inhibition of marine coastal bloom-forming phytoplankton by commercially cultivated *Gracilaria lemaneiformis* (Rhodophyta). J. Appl. Phycol. 27, 2341–2352. https://doi.org/10.1007/s10811-014-0486-0.

Yao, Y., Wang, C., 2022. Marine heatwaves and cold-spells in global coral reef zones. Prog. Oceanogr. 209, 102920. https://doi.org/10.1016/j.pocean.2022.102920.

Ye, Y., Zhang, L., Yang, R., Luo, Q., Chen, H., Yan, X., Tang, H., 2013. Metabolic phenotypes associated with high-temperature tolerance of *Porphyra haitanensis* strains. J. Agric. Food Chem. 61, 8356–8363. https://doi.org/10.1021/jf402749a.

Ye, C., Liao, H., Yang, Y., 2014. Allelopathic inhibition of photosynthesis in the red tide-causing marine alga, *Scrippsiella trochoidea* (Pyrrophyta), by the dried macroalga, *Gracilaria lemaneiformis* (Rhodophyta). J. Sea Res. 90, 10–15. https://doi.org/10.1016/j.seares.2014.02.015.

Yu, Q., Yu, Z.M., Song, X.X., Cao, X.H., Jiang, W.B., Chu, Y.Y., 2023. The synthesis of an acrylamide copolymer and its synergistic effects on clay flocculation of red tide organisms. J. Environ. Manag. 332, 117326. https://doi.org/10.1016/j.jenvman.2023.117326.

Zhang, B., Sun, D., Zhang, X., Sun, X., Xu, N., 2022. Transcriptomics and metabolomics reveal the adaptive mechanisms of *Gracilariopsis lemaneiformis* in response to blue light. Algal Res. 66, 102760. https://doi.org/10.1016/j.algal.2022.102760.